QUANTUM MECHANICS

Extending Wheeler's delayed-choice experiment to space

Francesco Vedovato,[1]* Costantino Agnesi,[1]* Matteo Schiavon,[1] Daniele Dequal,[1,2] Luca Calderaro,[1] Marco Tomasin,[1] Davide G. Marangon,[1] Andrea Stanco,[1] Vincenza Luceri,[3] Giuseppe Bianco,[2] Giuseppe Vallone,[1] Paolo Villoresi[1]†

Gedankenexperiments have consistently played a major role in the development of quantum theory. A paradigmatic example is Wheeler's delayed-choice experiment, a wave-particle duality test that cannot be fully understood using only classical concepts. We implement Wheeler's idea along a satellite-ground interferometer that extends for thousands of kilometers in space. We exploit temporal and polarization degrees of freedom of photons reflected by a fast-moving satellite equipped with retroreflecting mirrors. We observe the complementary wave- or particle-like behaviors at the ground station by choosing the measurement apparatus while the photons are propagating from the satellite to the ground. Our results confirm quantum mechanical predictions, demonstrating the need of the dual wave-particle interpretation at this unprecedented scale. Our work paves the way for novel applications of quantum mechanics in space links involving multiple photon degrees of freedom.

INTRODUCTION

Quantum communications in space enable the investigation of the basic principles of quantum mechanics in a radically new scenario. As envisioned in theoretical works (*1*–*6*) and satellite mission proposals (*7*–*9*), quantum information protocols (*10*, *11*) have breached the space frontier (*12*) in recent experimental demonstrations (*13*–*20*). These developments foster the implementation in space of fundamental tests of Physics, such as the Gedankenexperiments that highlight the counterintuitive aspects of quantum theory.

These thought experiments played a primary role in the famous debate between Einstein and Bohr (*21*), concerning the completeness of quantum mechanics (*22*, *23*) and the concept of complementarity (*24*). The most disturbing implication of complementarity is the wave-particle duality of quantum matter, which is the impossibility of revealing both the wave- and particle-like properties of a quantum object at the same time. Bohr pointed out that it is necessary to consider the whole apparatus to determine which property is measured, stating that there is no difference "whether our plans of constructing or handling the instruments are fixed beforehand or whether we postpone the completion of our planning until a later moment" (*21*).

John Wheeler pushed this observation to the extreme and conceived his delayed-choice Gedankenexperiment to highlight the contradictory interpretation given by classical physics (*25*, *26*). In his idea, a photon emerging from the first beam splitter (BS) of a Mach-Zehnder interferometer (MZI) (Fig. 1) may find two alternative configurations. Given the presence or absence of a second BS at the output of the interferometer, the apparatus measures the wave- or particle-like character of the photon. If the BS is absent, then only one of the two detectors will fire, reflecting the fact that the photon traveled along only one arm of the interferometer and revealing which path it took, as a classical particle would have done. If the BS is present, then interference can be observed, reflecting the fact that the photon traveled both routes, as a classical wave would have done.

If the configuration is chosen after the photon enters the interferometer, then a purely classical interpretation of the process in which the photon decides its nature at the first BS would imply a seeming violation of causality. On the other hand, in the quantum mechanical interpretation of the experiment, the photon maintains its dual wave-particle nature until the very end of the experiment, when it is detected.

Here, we extend the delayed-choice paradigm to space, as sketched in Fig. 1, by exploiting the temporal degree of freedom of photons reflected by a rapidly moving satellite in orbit. The two paths of the interferometer are represented by two time bins that allow us to both obtain clear which-path information and observe interference modulated by the satellite motion. We also exploit photon polarization as an ancillary degree of freedom to implement the insertion or removal of the BS at the measurement apparatus. We are able to demonstrate the need of the

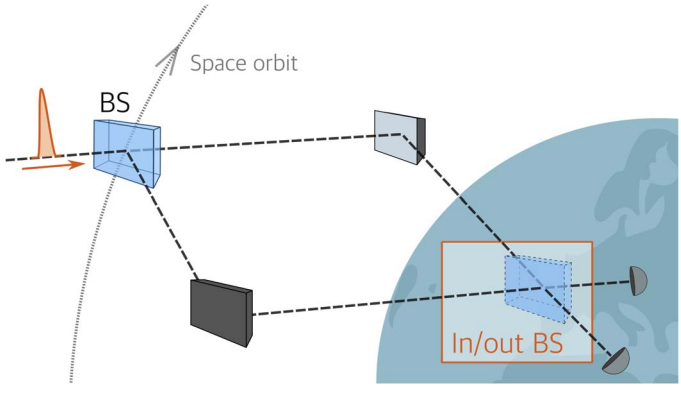

Fig. 1. Pictorial representation of Wheeler's delayed-choice experiment in space. A photon wave packet enters the first BS of an interferometer, which extends along thousands of kilometers in space. The interferometer can be randomly arranged according to two configurations that correspond to the presence or absence of the second BS (in/out BS) located on Earth. Following Wheeler's idea, the configuration choice is performed when the photon has already entered the interferometer. In our actual implementation, the interferometer begins and terminates on the ground, extending up to the target satellite, and the measurement choice performed on ground is space-like separated from the photon reflection by the satellite.

[1]Dipartimento di Ingegneria dell'Informazione, Università degli Studi di Padova, Padova, Italy. [2]Matera Laser Ranging Observatory, Agenzia Spaziale Italiana, Matera, Italy. [3]e-GEOS S.p.A., Matera, Italy.
*These authors contributed equally to this work.
†Corresponding author. Email: paolo.villoresi@dei.unipd.it

dual wave-particle model for a propagation distance of up to 3500 km, demonstrating the validity of the quantum mechanical description at a much larger scale than all previous experiments.

So far, several implementations of Wheeler's Gedankenexperiment have been realized on the ground [see the study of Jacques *et al.* (*27*) for the realization closest to the original idea and the study of Ma *et al.* (*28*) for a complete review]. An alternative way of interpreting the delayed-choice experiment is within the quantum-erasure framework (*29*, *30*). Furthermore, a quantum delayed-choice version of the experiment, where a quantum ancilla controls the second BS, has been recently proposed (*31*) and realized (*32*–*34*).

RESULTS

Description of the experiment

We realized the experiment at the Matera Laser Ranging Observatory (MLRO) of the Italian Space Agency. At the MLRO, we have already tested the feasibility of receiving qubits encoded in the polarization of single photons (*15*) and of observing interference between two temporal modes throughout satellite-ground channels in the study of Vallone *et al.* (*17*). A pulsed laser [repetition rate, 100 MHz; wavelength λ = 532 nm; energy per pulse, ~1nJ], diagonally polarized and paced by an atomic clock, enters into an unbalanced MZI, as sketched in Fig. 2. The combined action of the first polarizing BS (MZI-PBS) and of the imbalance of the MZI transforms each laser pulse into a superposition of two temporal and polarization modes. The long arm of the MZI is traveled by the vertically polarized component of the beam, whereas the horizontally polarized component travels along the short arm. The separation between the two temporal modes is about $\Delta t \approx 3.5$ ns (see Materials and Methods for more details).

The pulses then pass through two liquid crystal retarders (LCRs) whose combined action is equivalent to a single switchable (on/off) half–wave plate (sHWP) inclined at 45° with respect to the fast axis. During the transmission period, the sHWP is always off, leaving the outgoing beam unperturbed. The light is then directed to a target satellite equipped with polarization-maintaining corner-cube retroreflectors via a telescope (*15*). The corner cubes of the target satellite redirect the beam back to the ground station. Furthermore, the radial motion of the satellite introduces a kinematic phase shift between the two time bins given by

$$\varphi(t) = \frac{2\beta(t)}{1+\beta(t)}\,\frac{2\pi c}{\lambda}\,\Delta t \qquad (1)$$

where $\beta(t) = v_r(t)/c$, with $v_r(t)$ as the instantaneous satellite radial velocity with respect to the ground and c as the speed of light in vacuum, as demonstrated by our group in a previous study (*17*).

The photons returning from the satellite are collected by the same telescope and injected into the optical table, where they reencounter the same sHWP and MZI. At an exit port of the MZI-PBS (Fig. 2), we perform a polarization measurement in the diagonal and antidiagonal basis $\{|+\rangle, |-\rangle\}$ with $|\pm\rangle = (|H\rangle \pm |V\rangle)/\sqrt{2}$, where $|H\rangle, |V\rangle$ are the horizontal and vertical polarization states, respectively.

While the photons are propagating back to MLRO, an on-demand quantum random number generator (QRNG) extracts a random bit $b \in \{0, 1\}$ with a 50% probability. The QRNG is based on differences of the arrival time of single photons in attenuated light (*35*), and its relevant features will be detailed in Materials and Methods. The bit value sets the voltages V_b applied to the LCRs, determining the on or off behavior of the sHWP. The latter determines whether we perform a measurement that reveals the particle-like (sHWP on) or wave-like (sHWP off) behavior of the photons returning from the satellite. Because the random bits are generated while the photons are traveling from the satellite to the ground station, we ensure a space-like separation between the measurement choice and the last interaction with the apparatus, that is, the reflection by the satellite (as detailed in the "Implementation of the delayed choice" section).

Let us first suppose that the QRNG extracts a $b = 0$ bit causing the sHWP to remain off, leaving the polarization of the photon unchanged as it reenters the MZI. At the exit port of the MZI-PBS toward the detectors in Fig. 2, only the horizontally polarized component that propagated through the long arm and the vertically polarized component that traveled along the short arm can be detected. Because this is the reverse situation compared to the outward passage through the MZI, the two polarization modes will recombine into a single temporal mode, losing all which-path information and allowing us to observe a φ-dependent interference, which is the fingerprint of the wave-like nature of the photon. In this case, the probabilities of a click in the detectors $\mathrm{Det}_\pm$ are given by

$$P_\pm^{b=0}(t) = \frac{1}{2}[1 \pm \mathcal{V}(t)\cos\varphi(t)] \qquad (2)$$

where $\mathcal{V}(t) \approx 1$ is the theoretical visibility as in the study of Vallone *et al.* (*17*).

Let us now suppose that the QRNG extracts a $b = 1$ bit, switching the sHWP on and swapping the horizontal and vertical polarizations before the photon reenters the MZI. The polarization transformation causes each component of the state to retravel along the same arm compared to the outwards passage through the MZI. As a result, the photon can be detected at two distinct times separated by $2\Delta t$ (with 50% probability for each detector $\mathrm{Det}_\pm$, that is, $P_\pm^{b=1}(t) = 1/2$), giving which-path information and evidencing the particle-like nature of the photon.

Implementation of the delayed choice

Simultaneous tracking of the target satellite via the satellite laser ranging (SLR) technique allows the determination with few tens of picosecond accuracy of the photon's time of flight or round trip time (rtt). Furthermore, SLR allows an accurate estimation of the satellite radial velocity, which is crucial for the determination of the kinematic phase $\varphi(t)$. The laser ranging technique exploits a bright laser signal with pulses at a 10-Hz repetition rate, synchronized with the 100-MHz train used in the experiment (see Materials and Methods for more details).

We separated each 100-ms cycle between two subsequent SLR pulses in two periods by using two mechanical shutters (Figs. 2 and 3). In the first half of the 100 ms, only the transmitting shutter (TX shutter) is open, whereas the receiving one (RX shutter) is closed to protect the detectors. In the second half of the time slot, the TX shutter is closed, whereas the RX shutter is open, and the detectors can receive the photons coming from the satellite. Furthermore, because the shutters require a certain time to open and close completely, the effective detection time period is limited by the shutters transition time ($t_{\mathrm{trans}} \sim 5$ ms), as sketched in the figure. On that basis, a precise temporal window $\tau = \mathrm{rtt} - t_{\mathrm{trans}}$ exists, where we expect to receive photons from the satellite. The value of τ depends on the actual rtt, which is continuously changing along the satellite orbit. However, the SLR technique described above

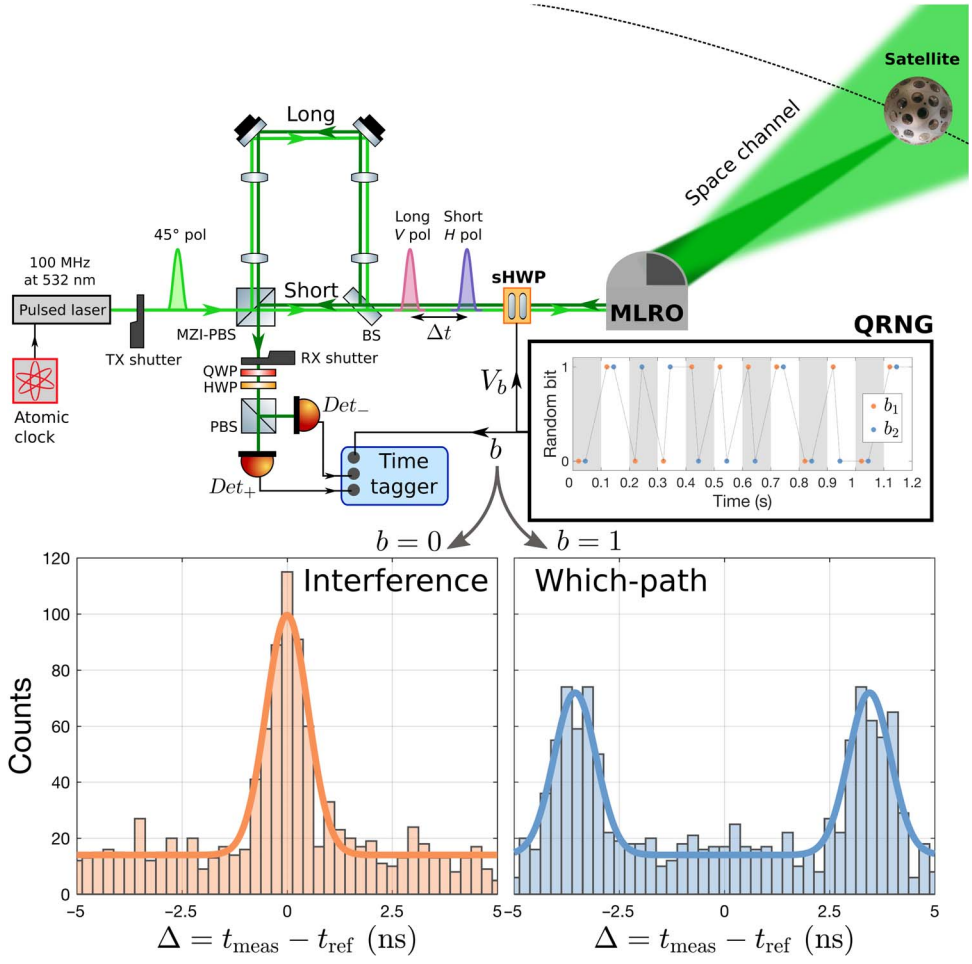

Fig. 2. Scheme of the experimental setup and detection histograms. A pulsed laser synchronized with the MLRO atomic clock exits the MZI in two temporal and polarization (pol) modes. The sHWP leaves the pulses unperturbed, and the telescope directs the beam to a target satellite. After the reflection, the photons are collected on the ground by the same telescope and injected into the optical table. The photons pass through the sHWP whose behavior is set according to the bit *b* extracted from an on-demand QRNG. The QRNG is inquired twice in each 100-ms cycle of the experiment, as detailed in the main text. In the inset, a 1-s sample of the extracted bits is shown. At the MZI output, two wave plates, a PBS, and two single-photon detectors (SPDs) perform a polarization measurement in the $\{|+\rangle, |-\rangle\}$ basis. According to the value *b* of the random bit, interference or which-path measurement is performed, as shown by the detection histograms for a passage of the Starlette satellite. The counts in the central peak on the left histogram are comparable to the sum of the counts associated to the lateral peaks on the right one, as expected. HWP, half–wave plate; QWP, quarter–wave plate.

allows the transmission and reception phases of the protocol to be synchronized in real time by using a fast field-programmable gate array (FPGA) controller.

A faithful realization of Wheeler's experiment requires that the entrance of the photon in the interferometer is not in the future light cone of the measurement choice. Moreover, the latter must be realized in a random manner: This prevents any causal influence of the measurement choice on the behavior of the photon.

Our implementation is performed over a space channel with a length of the order of thousands of kilometers, corresponding to an rtt of the order of 10 ms. We designed the experiment to guarantee that the choice of the measurement apparatus is space-like separated from the reflection of the photon from the satellite, as shown in the Minkowski diagram in Fig. 3. This guarantees that, in a purely classical interpretation, a photon "should have decided its nature" at most at its reflection from the satellite.

For each cycle, we performed two independent choices that will affect the detections in the acceptable temporal window τ by driving the QRNG with the same FPGA controller used for the shutters. The sHWP behavior at the photon return is set according to the bits b_1 and b_2 extracted by the QRNG. The first choice is performed at t_{b_1}, corresponding to the middle of the shutter transition phase.

The second choice is at t_{b_2}, which occurs with a delay rtt/2 with respect to the first choice. The detected photons are divided into two groups, each characterized by a value of the bit choice. In this way, all the photons of a given group were already reflected by the satellite when the corresponding bit choice was performed.

Measurement of complementary dual wave-particle properties

We selected the passages of two low-Earth-orbit (LEO) satellites equipped with polarization-maintaining corner-cube retroreflectors, namely,

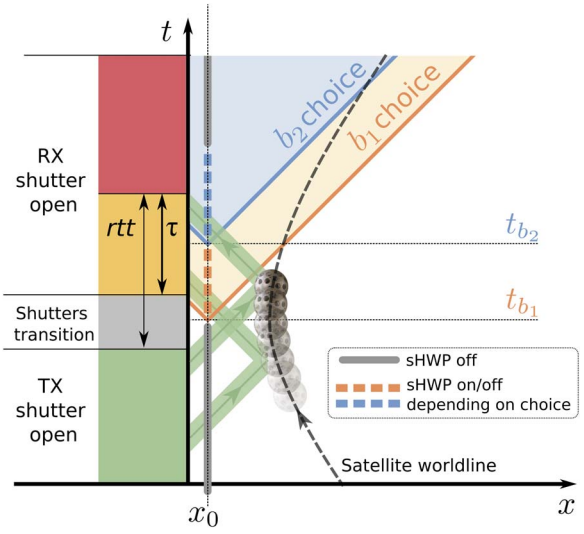

Fig. 3. Minkowski diagram of the experiment. Along the temporal axis (not to scale) a 100-ms cycle between two SLR pulses is represented. The *x* axis represents the radial coordinate (not to scale) from the detectors, where x_0 is the position of both the sHWP and the QRNG. The dotted line is the satellite worldline. We only considered the detections in the temporal window τ, as detailed in the main text. A fast FPGA controller synchronized in real time with the MLRO tracking system drives the two shutters and the QRNG. For each cycle, we performed two independent measurements via the random bit extracted by the QRNG at times t_{b_1} and t_{b_2}, causally disconnected from the photon reflection at the satellite. The cycle is repeated for each 100-MHz train between two SLR pulses.

Beacon-C dated 1 November 2016 23:18 CEST (Central European Summer Time) (with a slant distance ranging from 1264 to 1376 km with respect to the MLRO) and Starlette dated 1 November 2016 22:00 CEST (with a slant distance ranging from 1454 to 1771 km).

The synchronization between our signal and the bright laser-ranging pulses allowed us to predict the expected arrival time t_{ref} of the photons, which is not periodic along the orbit due to the satellite motion. The effective arrival time t_{meas} was tagged by a time-to-digital converter (Fig. 2, time tagger). Therefore, we may obtain a detection histogram as a function of the time difference $\Delta = t_{meas} - t_{ref}$ (Fig. 2, bottom) for the data recorded in the Det$_-$ detector in the passage of the Starlette satellite (results for the Det$_+$ are analogous).

As previously described, we separated the detections in two groups according to the setting of the sHWP. On the left histogram in Fig. 2, we gathered all the detections characterized by the bit value $b = 0$, and we obtained a single central peak, where the which-path information is erased and the interference effects should be observed. The peak width is determined mostly by the timing jitter of the detector, which is about 0.5 ns [root mean square (RMS)]. On the right histogram, the extracted bit *b* was equal to 1, and we obtained a histogram with two well-separated lateral peaks, manifesting the expected particle-like behavior. An indication of good assessment for the setup is given by the fact that the peak obtained when $b = 0$ is comparable with the sum of the two lateral peaks obtained when $b = 1$ because the number of "0" and "1" bits from the QRNG is balanced. We note that, even if interference is expected in the $b = 0$ case, it is not apparent in Fig. 2 because we are not taking into account the phase shift φ(*t*) introduced by the satellite, and thus, the interference effect is completely averaged over all the data.

To evaluate the role of the kinematic phase φ(*t*), these two data sets were further separated into 10 phase intervals (length, π/5 rad) defined by $I_j \equiv [(2j - 1)\pi/10, (2j + 1)\pi/10]$, where $j = 0,..., 9$. For each phase interval, we selected the detection events characterized by φ (mod $2\pi) \in I_j$. Then, for each selected data set, we evaluated the detection histogram as a function of the time difference Δ, as described above. These histograms were used to determine the photon counts $N_\pm$ by taking all the events recorded by Det$_\pm$ in a precise detection window centered at the expected arrival time of the photon. The width of the detection window (0.9 ns) was chosen to optimize the trade-off between signal-to-noise ratio and count rate. From the counts, we calculated the relative detection frequency $f_\pm = \eta_\mp N_\pm/(\eta_- N_+ + \eta_+ N_-)$, where $\eta_+ = 0.12$ and $\eta_- = 0.10$ account for the different quantum efficiencies of the detectors used. The resulting relative frequencies $f_\pm$ and their Poissonian errors are plotted in Fig. 4 for the two satellites.

For the "interference" subset of the data, we may observe the relative phase information by erasing the photon's "which-path" information. This is evident by the recovery of the interference pattern shown in Fig. 4 (left panels). By fitting the data with $P_\pm = (1 \pm \mathcal{V}_{exp} \cos\varphi)/2$ given by Eq. 2, we obtained an experimental visibility value $\mathcal{V}_{exp} \approx 40\%$ for both satellites and a clear phase-dependent modulation in the two detector outcomes. Furthermore, the visibility obtained during preliminary tests, where the sHWP was fixed in the off mode, is compatible with the results obtained while performing the delayed choice, attesting that the latter had no influence in the observed interference pattern. The value of the experimental visibility, lower than the theoretical value of 100%, is due to experimental imperfections in the MZI and residual birefringence caused by the telescope Coudé path mirrors. This result once more validates the theoretical model for the kinematic phase φ(*t*) introduced and exploited in our recent work (*17*).

On the other hand, the which-path relative frequencies are constant (within statistical fluctuations) for all values of φ, as predicted by the theoretical model $P_\pm = 1/2$. In this case, the which-path measurement destroys any information about the relative phase of the two time bins.

When the photon's particle-like nature is inquired, we obtain conclusive which-path information with probability $p_{wp} = 88 \pm 1\%$ ($86 \pm 1\%$) for Beacon-C (Starlette). These values are obtained by the ratio between the counts in the lateral peaks and the total ones: When the photon is detected in one of the two lateral peaks, the which-path information is recovered. Because classical particles should always give complete which-path information, we could naively conclude that our photons behave as classical particles for at least 86% of the time. If such interpretation were correct, then we would expect interference with at most 14% visibility when the photon's wave-like nature is inquired. This is in remarkable contrast with the measured visibility, which is at least 5σ distant from that prediction, allowing us to exclude any model where the photon behaves as a purely classical particle. Note that, to also rule out semiclassical theories in which the classical electromagnetic field interacts with quantized matter at the detection, true single photons should be used instead of attenuated light (*28*).

The agreement between the theoretical model and the obtained results can be assessed by calculating the residuals between the fit and the experimental data. We can observe that these residuals are randomly distributed within the foreseeable Poissonian fluctuations (Fig. 4). Most points lay within ± 1.5σ from the expected values, where σ is the mean error. This can also be seen by calculating the RMS of

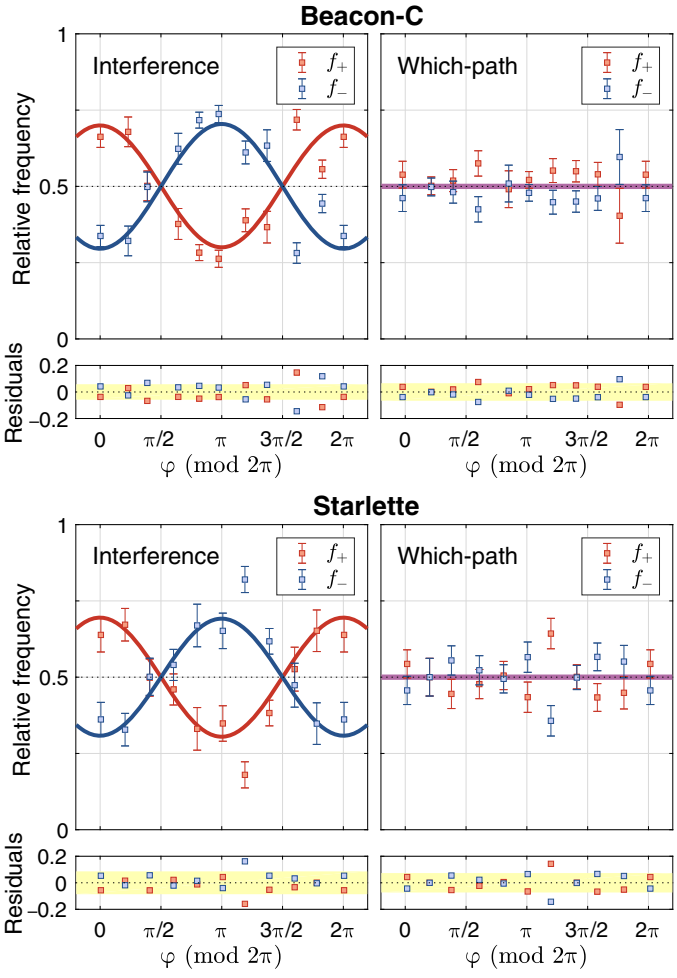

Fig. 4. Experimental results for the interference and which-path configurations. Relative frequencies $f_{\pm}$ of counts in the two detectors $\mathrm{Det}_{\pm}$ as a function of the kinematic phase φ introduced by the satellite for the passages of Beacon-C and Starlette satellites. The error bars are estimated using the Poissonian error associated to counts. We show the relative residuals as a function of φ below each plot. We note that, at the point $\varphi \approx 0$ and $\varphi \approx 2\pi$, the same subset of data was selected. In the interference configuration, we estimated a visibility $\mathcal{V}^{B} = 40 \pm 5\%$ for Beacon-C and $\mathcal{V}^{S} = 39 \pm 4\%$ for Starlette from the fitted data.

the residuals $\sigma_R \sim 0.05$ for both satellites, which is compatible with the expected statistical fluctuations.

Given the optical losses $\eta_{opt} \approx 0.13$ in the receiving setup and the detection efficiency $\eta_{det} \approx 0.1$, the mean number of photons μ in the received pulses can be derived by measuring the detection rate. At the primary mirror, we received $\mu \approx 2.2 \times 10^{-3}$ for Starlette and $\mu \approx 1.9 \times 10^{-3}$ for Beacon-C. From these values, we can conclude that the particle- and wave-like properties are measured at the single-photon level because the probability of having more than one photon per pulse passing through the MZI on the way back is $\sim\mu^2/2$, which is, at most, of the order of 10^{-6}.

DISCUSSION

We realized Wheeler's delayed-choice Gedankenexperiment along a space channel involving LEO satellites by combining two independent degrees of freedom of light. The experimental arrangement that allows the measurement of the complimentary wave or particle behaviors of light quanta was randomly set according to two alternative configurations while the photons were already inside the apparatus, as required in the delayed-choice paradigm. To measure interference with the first configuration, it is crucial to take into account the kinematic phase shift introduced by the satellite motion. By observing single-photon interference after the propagation along a 3500-km space channel, we can confute with clear statistical evidence of 5σ the description of light quanta as classical particles. In the alternative configuration of the detection scheme, the phase-dependent modulation in the received clicks disappears, and the which-path information can be clearly reconstructed.

The high losses in the two-way propagation between the ground station and the satellite hampers the implementation of this scheme for the delayed-choice experiments using true single-photon sources or entangled particles, such as delayed-choice quantum erasure and entanglement swapping (*36*). These experiments, already demonstrated on the ground (*28*, *34*, *37*), require an active source on a satellite for the implementation in the space scenario.

Our results extend the validity of the quantum mechanical description of complementarity to the spatial scale of LEO orbits. Furthermore, they support the feasibility of efficient encoding by exploiting both polarization and time bin for high-dimensional free-space quantum key distribution (*38*) over long distances. Finally, our work paves the way for satellite implementation of other foundational-like tests and applications of quantum mechanics involving hyper-entangled states (*39*–*42*), around the planet and beyond.

MATERIALS AND METHODS

Experimental design

The laser pulse train used in the delayed-choice experiment was generated by a Nd:YVO_4 mode-locking master oscillator paced by an atomic clock and stabilized at a repetition rate of 100 MHz, corresponding to a temporal separation between the pulses of 10 ns. The 1064-nm pulses were then up-converted to the desired wavelength λ = 532 nm with a 5-cm-long periodically poled lithium niobate crystal (HC Photonics). The mean power of the train was of the order of 100 mW, corresponding to an energy per pulse of 1 nJ. The beam was sent through a bulk MZI with an imbalance of about 1 m, where in the long arm, two 4*f* relaying optical systems guaranteed the matching of the beam wave fronts. To mitigate optical aberration, we designed each 4*f* system by using two doublets (meniscus and plano convex lens) of equivalent focal length of about 125 mm.

We measured the temporal imbalance Δ*t* of the MZI by sending the pulsed train through it and using a single-photon avalanche photodiode (PDM, Micro Photon Devices) in one of the BS output ports. As expected, the detections appeared at two different times in two well-separated peaks. Each peak was characterized by an exponentially modified Gaussian distribution whose standard deviation was of the order of 40 ps (due to the timing jitter of the detector and the pulse duration). By fitting the distribution, we estimated the imbalance of the MZI as $\Delta t = 3.498 \pm 0.002$ ns.

The sHWP was composed of two LCRs mounted with orthogonal axes. Each LCR introduced phase retardation between the two orthogonal polarization modes of the impinging light, depending on the applied voltage. We characterized the two LCRs by measuring the birefringence introduced as a function of the applied voltage and then designed the two LCRs to act as a single fast-switching HWP inclined at 45°. With this configuration, we obtained a switching time $t_{sHWP} \lesssim 500$ μs.

The 100-MHz train was directed via a Coudé path to the satellite through the 1.5-m diffraction-limited Cassegrain telescope of MLRO, which has been designed for SLR (*43*). The highly directive back-reflection of the corner cubes mounted on the satellites dedicated to ranging, as for those used in experiment, was then collected by MLRO and directed back to the MZI.

At the MZI-PBS output port, the beam was focused and spectrally filtered before passing through a QWP, HWP, and the PBS that performed the polarization measurement in the $\{|+\rangle, |-\rangle\}$ basis. The photons were finally collected by two single-photon photomultipliers (detection efficiency, ~10%; active diameter, 22 mm; H7360-02, Hamamatsu Photonics) whose detection times were recorded by a time-to-digital converter (QuTau time tagger, Qutools) with a resolution of 81 ps. The time tagger also stored the encoded value of bit b extracted by the QRNG.

To determine the expected arrival time t_{ref} of the reflected pulses and to estimate the value $\varphi(t)$ of the kinematic phase shift introduced by the satellite, the 100-MHz train was synchronized to a strong 10-Hz laser train used for SLR. The SLR train was generated by the same mode-locking master oscillator used for the 100-MHz train by selecting one pulse every 10^7. Each SLR pulse was then amplified and up-converted by a second-harmonic generation stage resulting in an SLR train at 532 nm with 1 W of mean power (corresponding to an energy of 100 mJ per pulse at a repetition rate of 10 Hz). A BS was used for combining the two pulsed beams before sending them to the target satellite via the MLRO telescope.

By taking into account the Doppler effect, we can estimate the instantaneous radial velocity with respect to the ground station $v_r(t) = \frac{c(\Delta T' - \Delta T)}{\Delta T' + \Delta T}$, where $\Delta T'$ is the temporal separation of two consecutive SLR pulses in reception and $\Delta T = 1/(10\ \mathrm{Hz}) = 100$ ms is the temporal separation of two consecutive SLR pulses in transmission (*44*). This information is crucial for the estimation of the kinematic phase shift introduced by the satellite because it is continuously changing along the orbit.

Quantum random number generator

The QRNG device generates random numbers on demand by using a protocol based on the differences of the times of arrival of single photons in attenuated light (*35*). This protocol requires a light source (a light-emitting diode in our case) attenuated to single-photon level and only one SPD. The device was realized with the FPGA technology for a full control over the time evolution of the generation process and for the integration with the data acquisition at MLRO. As described in the main text, our implementation of Wheeler's experiment requires two random bits b_1 and b_2 at specific times t_{b_1} and t_{b_2} (separated by rtt/2) to set the sHWP in each 100-ms cycle. Because the QRNG has an average latency in the random bit generation of about 20 μs and the sHWP requires ~500 μs at most to change its state, the setup guarantees that the time from the inquiry of the QRNG to the generation of the random bit and the subsequent setting of the sHWP is much shorter than rtt/2. In the experiment, we used two identical QRNG setups (two light sources, two SPDs, and two FPGA architectures) and combined the two outputs with an XOR operation to extend the total entropy value and add robustness to the design. The QRNG final bit stream has a bias value (10^{-4} in a 100-megabit string) and correlation values of the first 100 lags between -2.5×10^{-4} and 2.5×10^{-4}. These values fulfill the statistical requirements for high-quality on-demand QRNG, guaranteeing the randomness of the output bits. The timing of the experiment ensures the required relativistic space-like separation between the bit extraction and the photon reflection at the satellite, as described in the main text.

REFERENCES AND NOTES

1. J. G. Rarity, P. R. Tapster, P. M. Gorman, P. Knight, Ground to satellite secure key exchange using quantum cryptography. *New J. Phys.* **4**, 82 (2002).
2. M. Aspelmeyer, T. Jennewein, M. Pfennigbauer, W. R. Leeb, A. Zeilinger, Long-distance quantum communication with entangled photons using satellites. *IEEE J. Sel. Top. Quantum Electron.* **9**, 1541–1551 (2003).
3. A. Tomaello, C. Bonato, V. Da Deppo, G. Naletto, P. Villoresi, Link budget and back-ground noise for satellite quantum key distribution. *Adv. Space Res.* **47**, 802–810 (2011).
4. D. Rideout, T. Jennewein, G. Amelino-Camelia, T. F. Demarie, B. L. Higgins, A. Kempf, A. Kent, R. Laflamme, X. Ma, R. B. Mann, E. Martín-Martínez, N. C. Menicucci, J. Moffat, C. Simon, R. Sorkin, L. Smolin, D. R. Terno, Fundamental quantum optics experiments conceivable with satellites-reaching relativistic distances and velocities. *Classical Quantum Gravity* **29**, 224011 (2012).
5. J. P. Bourgoin, E. Meyer-Scott, B. L. Higgins, B. Helou, C. Erven, H. Hübel, B. Kumar, D. Hudson, I. D'Souza, R. Girard, R. Laflamme, T. Jennewein, A comprehensive design and performance analysis of low Earth orbit satellite quantum communication. *New J. Phys.* **15**, 023006 (2013).
6. D. E. Bruschi, T. C. Ralph, I. Fuentes, T. Jennewein, M. Razavi, Spacetime effects on satellite-based quantum communications. *Phys. Rev. D* **90**, 045041 (2014).
7. R. Ursin, T. Jennewein, J. Kofler, J. M. Perdigues, L. Cacciapuoti, C. J. de Matos, M. Aspelmeyer, A. Valencia, T. Scheidl, A. Acin, C. Barbieri, G. Bianco, C. Brukner, J. Capmany, S. Cova, D. Giggenbach, W. Leeb, R. H. Hadfield, R. Laflamme, N. Lütkenhaus, G. Milburn, M. Peev, T. Ralph, J. Rarity, R. Renner, E. Samain, N. Solomos, W. Tittel, J. P. Torres, M. Toyoshima, A. Ortigosa-Blanch, V. Pruneri, P. Villoresi, I. Walmsley, G. Weihs, H. Weinfurter, M. Zukowski, A. Zeilinger, Space-quest, experiments with quantum entanglement in space. *Europhys. News* **40**, 26–29 (2009).
8. T. Scheidl, E. Wille, R. Ursin, Quantum optics experiments using the International Space Station: A proposal. *New J. Phys.* **15**, 043008 (2013).
9. T. Jennewein, C. Grant, E. Choi, C. Pugh, C. Holloway, J. P. Bourgoin, H. Hakima, B. Higgins, R. Zee, The NanoQEY mission: Ground to space quantum key and entanglement distribution using a nanosatellite. *Proc. SPIE* **9254**, 925402 (2014).
10. M. A. Nielsen, I. L. Chuang, *Quantum Computation and Quantum Information: 10th Anniversary Edition* (Cambridge Univ. Press, 2010).
11. N. Gisin, R. Thew, Quantum Communication. *Nat. Photon.* **1**, 165–171 (2007).
12. Quantum optics lifts off. *Nat. Photon.* **10**, 689 (2016).
13. P. Villoresi, T. Jennewein, F. Tamburini, M. Aspelmeyer, C. Bonato, R. Ursin, C. Pernechele, V. Luceri, G. Bianco, A. Zeilinger, Experimental verification of the feasibility of a quantum channel between space and Earth. *New J. Phys.* **10**, 033038 (2008).
14. J. Yin, Y. Cao, S.-B. Liu, G.-S. Pan, J.-H. Wang, T. Yang, Z.-P. Zhang, F.-M. Yang, Y.-A. Chen, C.-Z. Peng, J.-W. Pan, Experimental quasi-single-photon transmission from satellite to earth. *Opt. Express* **21**, 20032–20040 (2013).
15. G. Vallone, D. Bacco, D. Dequal, S. Gaiarin, V. Luceri, G. Bianco, P. Villoresi, Experimental satellite quantum communications. *Phys. Rev. Lett.* **115**, 040502 (2015).
16. D. Dequal, G. Vallone, D. Bacco, S. Gaiarin, V. Luceri, G. Bianco, P. Villoresi, Experimental single-photon exchange along a space link of 7000 km. *Phys. Rev. A* **93**, 010301(R) (2016).
17. G. Vallone, D. Dequal, M. Tomasin, F. Vedovato, M. Schiavon, V. Luceri, G. Bianco, P. Villoresi, Interference at the single photon level along satellite-ground channels. *Phys. Rev. Lett.* **116**, 253601 (2016).
18. Z. Tang, R. Chandrasekara, Y. C. Tan, C. Cheng, L. Sha, G. C. Hiang, D. K. L. Oi, A. Ling, Generation and analysis of correlated pairs of photons aboard a nanosatellite. *Phys. Rev. Appl.* **5**, 054022 (2016).
19. K. Günthner, I. Khan, D. Elser, B. Stiller, Ö. Bayraktar, C. R. Müller, K. Saucke, D. Tröndle, F. Heine, S. Seel, P. Greulich, H. Zech, B. Gütlich, S. Philipp-May, C. Marquardt, G. Leuchs, Quantum-limited measurements of optical signals from a geostationary satellite. *Optica* **4**, 611–616 (2017).
20. J. Yin, Y. Cao, Y.-H. Li, S.-K. Liao, L. Zhang, J.-G. Ren, W.-Q. Cai, W.-Y. Liu, B. Li, H. Dai, G.-B. Li, Q.-M. Lu, Y.-H. Gong, Y. Xu, S.-L. Li, F.-Z. Li, Y.-Y. Yin, Z.-Q. Jiang, M. Li, J.-J. Jia, G. Ren, D. He, Y.-L. Zhou, X.-X. Zhang, N. Wang, X. Chang, Z.-C. Zhu, N.-L. Liu, Y.-A. Chen, C.-Y. Lu, R. Shu, C.-Z. Peng, J.-Y. Wang, J.-W. Pan, Satellite-based entanglement distribution over 1200 kilometers. *Science* **356**, 1140–1144 (2017).
21. N. Bohr, Discussion with Einstein on epistemological problems in atomic physics, in *Quantum Theory and Measurement*, J. A. Wheeler, W. H. Zurek, Eds. (Princeton Univ. Press, 1984), pp. 9–49.

22. A. Einstein, B. Podolsky, N. Rosen, Can quantum mechanical description of physical reality be considered complete? *Phys. Rev.* **47**, 777–780 (1935).
23. N. Bohr, Can quantum-mechanical description of physical reality be considered complete? *Phys. Rev.* **48**, 696–702 (1935).
24. N. Bohr, The quantum postulate and the recent development of atomic theory. *Nature* **121**, 580–590 (1928).
25. J. A. Wheeler, The "past" and the "delayed-choice" double-slit experiment, in *Mathematical Foundations of Quantum Theory*, A. R. Marlow, Ed. (Academic Press, 1978), pp. 9–48.
26. J. A. Wheeler, Law without law, in *Quantum Theory and Measurement*, J. A. Wheeler, W. H. Zurek, Eds. (Princeton Univ. Press, 1984), pp. 182–213.
27. V. Jacques, E Wu, F. Grosshans, F. Treussart, P. Grangier, A. Aspect, J.-F. Roch, Experimental realization of Wheeler's delayed-choice gedanken experiment. *Science* **315**, 966–968 (2007).
28. X.-s. Ma, J. Kofler, A. Zeilinger, Delayed-choice gedanken experiments and their realizations. *Rev. Mod. Phys.* **88**, 015005 (2016).
29. M. O. Scully, K. Drühl, Quantum eraser: A proposed photon correlation experiment concerning observation and "delayed choice" in quantum mechanics. *Phys. Rev. A* **25**, 2208–2213 (1982).
30. M. O. Scully, B.-G. Englert, H. Walther, Quantum optical tests of complementarity. *Nature* **351**, 111–116 (1991).
31. R. Ionicioiu, D. R. Terno, Proposal for a quantum delayed-choice experiment. *Phys. Rev. Lett.* **107**, 230406 (2011).
32. J.-S. Tang, Y.-L. Li, X.-Y. Xu, G.-Y. Xiang, C.-F. Li, G.-C. Guo, Realization of quantum Wheelers delayed-choice experiment. *Nat. Photon.* **6**, 600–604 (2012).
33. A. Peruzzo, P. Shadbolt, N. Brunner, S. Popescu, J. L. O'Brien, A quantum delayed-choice experiment. *Science* **338**, 634–637 (2012).
34. F. Kaiser, T. Coudreau, P. Milman, D. B. Ostrowsky, S. Tanzilli, Entanglement-enabled delayed-choice experiment. *Science* **338**, 637–640 (2012).
35. M. Stipčević, B. M. Rogina, Quantum random number generator based on photonic emission in semiconductors. *Rev. Sci. Instrum.* **78**, 045104 (2007).
36. M. Żukowski, A. Zeilinger, M. A. Horne, A. K. Ekert, "Event-ready-detectors" Bell experiment via entanglement swapping. *Phys. Rev. Lett.* **71**, 4287–4290 (1993).
37. X.-s. Ma, S. Zotter, J. Kofler, R. Ursin, T. Jennewein, Č. Brukner, A. Zeilinger, Experimental delayed-choice entanglement swapping. *Nat. Phys.* **8**, 479–484 (2012).
38. T. Zhong, H. Zhou, R. Horansky, C. Lee, V. B. Verma, A. E. Lita, A. Restelli, J. C. Bienfang, R. P. Mirin, T. Gerrits, S. W. Nam, F. Marsili, M. D. Shaw, Z. Zhang, L. Wang, D. Englund, G. W. Wornell, J. H. Shapiro, F. N. C. Wong, Photon-efficient high-dimensional quantum key distribution. *New J. Phys.* **17**, 022002 (2015).
39. A. Cabello, Bipartite bell inequalities for hyperentangled states. *Phys. Rev. Lett.* **97**, 140406 (2006).
40. M. Barbieri, F. De Martini, P. Mataloni, G. Vallone, A. Cabello, Enhancing the violation of the Einstein-Podolsky-Rosen local realism by quantum hyper-entanglement. *Phys. Rev. Lett.* **97**, 140407 (2006).
41. T. Graham, C. Zeitler, J. Chapman, P. Kwiat, H. Javadi, H. Bernstein, Superdense teleportation and quantum key distribution for space applications, *2015 IEEE International Conference on Space Optical Systems and Applications (ICSOS 2016)*, New Orleans, LA, 26 to 28 October 2015.
42. F. Steinlechner, S. Ecker, M. Fink, B. Liu, J. Bavaresco, M. Huber, T. Scheidl, R. Ursin, Distribution of high-dimensional entanglement via an intra-city free-space link. *Nat. Commun.* **8**, 15971 (2017).
43. G. Bianco, R. Devoti, V. Luceri, C. Sciarretta, A review of Slr contributions to geophysics in Eurasia by Cgs. *Surv. Geophys.* **22**, 481–490 (2001).
44. G. Vallone, D. Dequal, M. Tomasin, M. Schiavon, F. Vedovato, D. Bacco, S. Gaiarin, G. Bianco, V. Luceri, P. Villoresi, Satellite quantum communication towards GEO distances. *Proc. SPIE* **9900**, 99000J (2016).

Acknowledgments: We thank F. Schiavone and G. Nicoletti of e-GEOS and the MLRO technical operators for the collaboration and support, G. Pantaleoni for his contributions to the setup and modeling during his Master's thesis at the University of Padova, and E. Vedovato for graphical support. **Funding:** This study was partially supported by the Strategic-Research-Project QUINTET of the Department of Information Engineering, University of Padova and the Strategic-Research-Project QUANTUMFUTURE of the University of Padova. F.V., L.C., and M.S. acknowledge the Center of Studies and Activities for Space "Giuseppe Colombo" for financial support. **Author contributions:** P.V. and G.V. conceived and supervised the experiment. P.V., G.V., F.V., C.A., M.T., and D.D. designed and tested the optical setup. P.V., G.V., D.D., L.C., F.V., C.A., M.S., V.L., and G.B. took part in the data acquisition at the MLRO. A.S., D.G.M., and D.D. implemented the QRNG. F.V., C.A., L.C., M.S., and D.D. analyzed the data. All authors contributed in writing the manuscript. **Competing interests:** The authors declare that they have no competing interests. **Data and materials availability:** All data needed to evaluate the conclusions in the paper are present in the paper. Additional data related to this paper may be requested from the authors.

Submitted 18 April 2017
Accepted 3 October 2017
Published 25 October 2017
10.1126/sciadv.1701180

Citation: F. Vedovato, C. Agnesi, M. Schiavon, D. Dequal, L. Calderaro, M. Tomasin, D. G. Marangon, A. Stanco, V. Luceri, G. Bianco, G. Vallone, P. Villoresi, Extending Wheeler's delayed-choice experiment to space. *Sci. Adv.* **3**, e1701180 (2017).

Extending Wheeler's delayed-choice experiment to space

Francesco Vedovato, Costantino Agnesi, Matteo Schiavon, Daniele Dequal, Luca Calderaro, Marco Tomasin, Davide G. Marangon, Andrea Stanco, Vincenza Luceri, Giuseppe Bianco, Giuseppe Vallone and Paolo Villoresi

Sci Adv **3** (10), e1701180.
DOI: 10.1126/sciadv.1701180